Structural Durability & Health Monitoring

Tech Science Press

Kinematic Analysis and Rock Mass Classifications for Rock Slope Failure at USAID Highways

Ibnu Rusydy[1,3,*], Nafisah Al-Huda[1,2], M. Fahmi[4] and Naufal Effendi[4]

[1]Department of Geological Engineering, Faculty of Engineering, Universitas Syiah Kuala, Banda Aceh, Indonesia
[2]Department of Civil Engineering, Faculty of Engineering, Universitas Syiah Kuala, Banda Aceh, Indonesia
[3]Tsunami and Disaster Mitigation Research Center (TDMRC), Universitas Syiah Kuala, Banda Aceh, Indonesia
[4]Department of Mining Engineering, Faculty of Engineering, Universitas Syiah Kuala, Banda Aceh, Indonesia
*Corresponding Author: Ibnu Rusydy. Email: ibnu@unsyiah.ac.id

Abstract: Rock slope kinematic analysis and rock mass classifications has been conducted at the 17th km to 26th km of USAID (United States Agency for International Development) highway in Indonesia. This research aimed to examine the type of rock slope failures and the quality of rock mass as well. The scan-line method was performed in six slopes by using a geological compass to determine rock mass structure on the rock slope, and the condition of joints such as persistence, aperture, roughness, infilling material, weathering and groundwater conditions. Slope kinematic analysis was performed employing a stereographic projection. The rock slope quality and stability were investigated based on RMR (rock mass rating) and SMR (slope mass rating) parameters. The rock slope kinematic analysis revealed that planar failure was likely to occur in Slope 1, 3, and 4, the wedge failure in Slope 1 and 6, and toppling failure in Slope 2, 5, and 6. The RMR rating is ranging from 57 to 64 and can be categorized as Fair to Good rock. The SMR rating revealed that the failure probability of Slope 3 was 90%, while it was from 40% to 60% for others. Despite the uniform RMR for all slopes, the SMR was significantly different. The detailed quantitative consideration of orientation of joint sets and geometry of the slope contributed to such differences in outcomes.

Keywords: Engineering geology; kinematic analysis; rock mass classifications; rock slope stability; Aceh; Indonesia

1 Introduction

Aceh province, located in the west of Indonesia, is a tectonically active area and its rocks are exposed to a high degree of weathering, and a high degree of fracturing of the rock mass. Consequently, this province is vulnerable to rock slope failures. Slope stability assessment is an essential factor to prevent slope failure, especially along road cut slopes. A few months following the Indian Ocean tsunami 2004, US government, deputized by USAID (United States Agency for International Development), contributed to Aceh province as part of the rehabilitation and reconstruction programs. One of the vast benefits to Acehnese was the 150 km western coast highway started from Banda Aceh to Calang, Aceh Jaya district. During the construction process of this highway, USAID's consultants and contractors cut through several hills and exposed the rock slopes beside the highway where rock falls recently occurred. These incidents have alerted many researchers to research and discover the appropriate solution to prevent this hazard; thus, the rock slope analysis is necessary. Rock slope stability problems have attracted rock engineer to propose several methods to analyse the rock slope stability such as rock slope kinematic analysis, limit equilibrium, numerical modelling, empirical approach, and rock mass classification [6, 29].

The structural geology features will affect the quality of the rock mass [14, 24, 27-29, 34]. These geological structures can be in the form of discontinuity planes, such as beddings, joints, folding, faults, and fractures. The quality of the rock governs the rock slope stability; hence, it can be examined by using the rock engineering approach, such as rock slope kinematic analysis and rock mass classifications. Many researchers, such as Basahel & Mitri [6], Gurocak et al. [15], Lee & Wang [19], Pantelidis [24], Rusydy et al. [27], Siddique et al. [29], have implemented these methods and have successfully analysed the quality and the stability of the rock slopes.

The rock slope in the study areas consisted of argillaceous limestone that were highly fractured and folded by tectonic forces. This limestone had been formed since Jurassic to Cretaceous and can be found along mountain ranges in Aceh province [3, 4]. Barber & Crow [4] recognized these limestone as accretion zone which were highly fractured by tectonic force in the geological time. Rusydy, et al. [27] noted that these limestones are blocky, disturbed-folded, and bedded, leading to being vulnerable to fail. The numbers of rock slope failures have recently occurred in this area, and thus slope stability analysis is of great concern. This research aimed to determine the typologies of rock slope failures and to study the rock mass quality to calculate the stability of rock slope. This rock quality data and kinematic analysis are the crucial parameters in rock slope engineering design and rock slope stability.

2 Tectonic Setting of Along the Slopes

The study area were located in the west coast highway of Aceh provinces, at the tip of Sumatra Island, the western part of Indonesia archipelago (see Fig. 1). The subduction zone in south-western of Sumatra, an interaction between Indo-Australian and Eurasia plates, influences the tectonic setting of this area [20, 21, 30]. The Indo-Australian move northward and it is subducted beneath the Eurasia plate approximately 5 cm per year [20].

The oblique convergence mechanism between the two plates leads to the Great Sumatra Fault (GSF) as the right-lateral fault systems running over 1900 km from Sunda Strait to Aceh province [20, 30], also reaching Andaman Sea. The subduction zone and GSF completely control the rock structures in Sumatra Island, creating folds, fractures, thrust-belt at the tip of Sumatra Island [11]. The structural geology in rock engineering, known as the discontinuity planes, including folds, faults, bedding, fractures, and joints, will influence the quality of the rock mass and the rock stability [14, 27, 28, 34].

Rock slopes in the investigation area were located several kilometres from Great Sumatra fault. The type of rock in these area is limestone and the structure is highly controlled by the fault system. Barber [3] and Barber & Crow [4], argued that the limestone in these areas were formed in the latest Jurassic to early Cretaceous period and was part of Gondwanaland. Barber [3], Barber & Crow [4], and Bennet, et al. [7], noted this Limestone as the argillaceous and siliceous limestone and part of Raba formation of Woyla group. These limestone are also known as the accretion sediment formed in the oceanic floor that are extremely fractured and folded by tectonic forces [27].

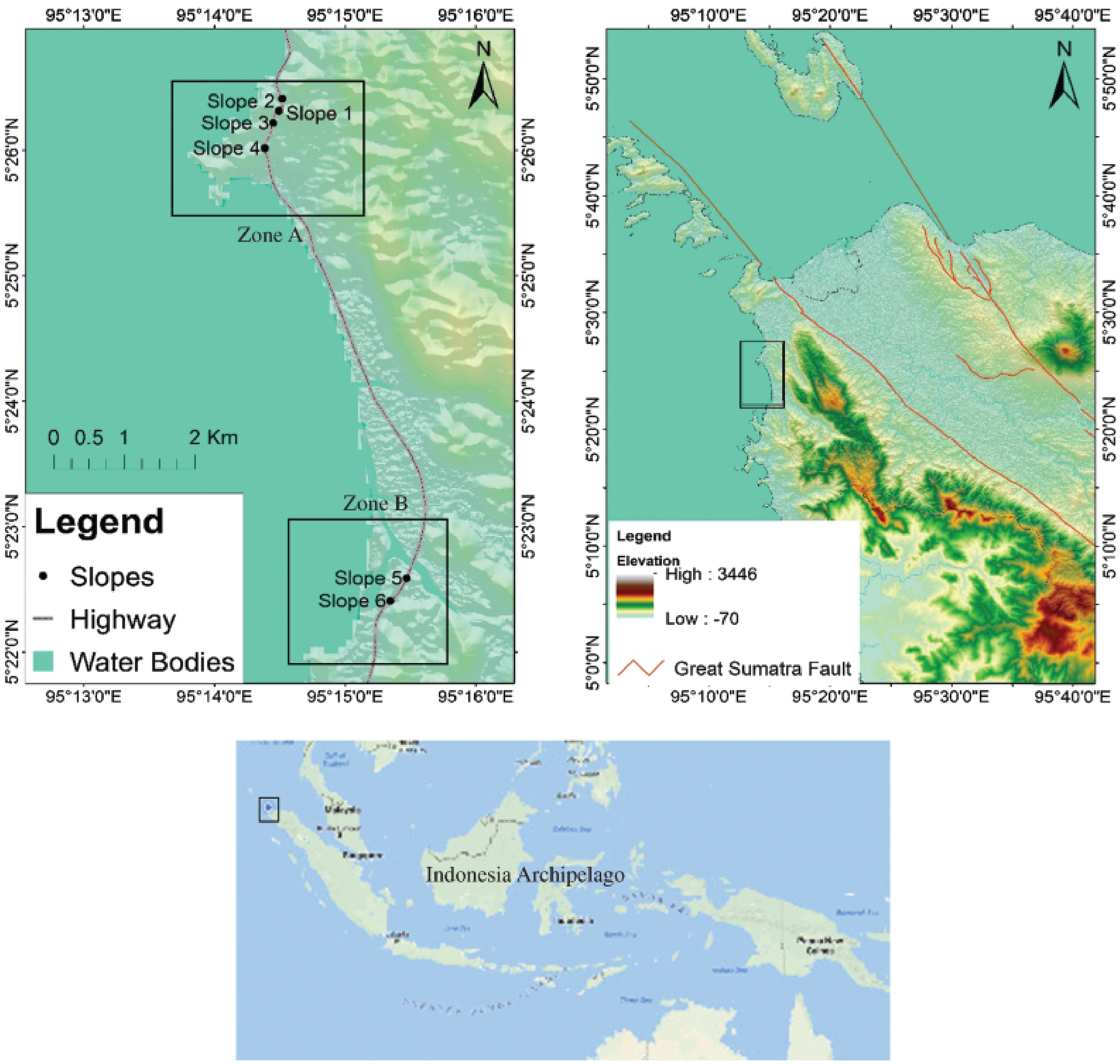

Figure 1: The locations of investigated road cut slopes at the tip of Sumatra Island, Indonesia, Digital elevation model derived from BIG 2018

3 Methods

The rock slope kinematic analysis and rock mass classifications were adopted in this study to determine the typologies of rock slope failures based on the stereography interpretation, and to convey a basic knowledge for empirical designs. Both methods have been widely used in rock engineering (civil and mining) to determine the quality of the rock mass. The classifications were called as the quantitative rock mass classification systems for rock engineering purpose. Rock mass classifications were conducted to evaluate the rock cutting performance based on the structural and inherent parameters [24]. Data collection concerning the rock slope kinematic analysis and the rock mass classifications were undertaken using the scan-line method, more details presented in the following section.

Rock mass classification was firstly developed by Ritter in 1878 by applying the empirical approach in tunnelling design, especially for supporting system [25]. The classifications are labelled as the quantitative rock mass classification system to connect and provide reliable communication between geologist, contractor, project designers, and civil engineers. In rock engineering practices, the most widely used rock mass classifications include RMR (rock mass rating) system developed by Bieniawski [8], the Q-system of Barton, et al. [5], the GSI (geological strength index) established by Hoek and Brown [18], and SMR (slope mass rating) for slope stability classification from Romana [26]. Recently, rock mass classifications had been widely used for civil and mining projects in rock engineering. However, this research only employed RMR and SMR.

3.1 Rock Slope Kinematic Analysis

Kinematic analysis refers to the movement of the materials without taking into account the forces causing the movement [15, 27]. The rock slope kinematic analysis carried out in this research was able to determine the type of possible failures or movement without considering the shear strength and resistance working on the rock slope. At this stage, the rock slope kinematic analysis is unable to produce the limit equilibrium analysis to define the safety factors.

Hoek & Bray [17] and Goodman [13] first introduced rock slope kinematic analysis. The analysis and calculation operate based on the stereographic projection method by inputting the dip and the dip direction/strike of the discontinuity planes from the field measurement using a geological compass [6, 27]. The stereographic projection approach is a method to project 3D into 2D geological structures [27]. The rock slope kinematic analysis enabled this study to analyse the slope and tunnel stability and determine the type of failures on the rock slope [19].

The scan-line method was utilized to investigate the rock mass structure in the maximum length of 50 meters for six slopes. The rock slope kinematic analysis proposed by Hoek & Bray [17] and Goodman [13] run on the stereographic projection analysis; the input data were the dip and the dip direction or the strike of the joints obtained from the field data by employing the geological compass [6, 27]. The stereographic projection is a technique to project the 3D geological structure into 2D and it requires imaginary interpretation [27]. The basic friction angle (*Φ)* plays a crucial role in the kinematic analysis; hence, this study adopted the tilt testing measurement developed by Ghani, et al [12], improved by Alejano, et al [1] and recommended by Hoek [16]. The Orient software from Vollmer [33] was used to display the joints orientation (the dip and its direction) and the slope geometry (the slope face angle and direction). Kamb contouring method developed by Vollmer [32] was performed to generate the contour in the stereography, as as result, the joint sets can be determined. Hoek & Bray [17] and Goodman [13] noted four types of slope failures in the rock slope kinematic analysis including: rotational, planar, wedge, and toppling (see Fig. 2). All those failures are possible to recognize from the stereography plot in Orient software.

3.1.1 The Plane Failure

A plane failure relatively in rock slopes when certain the geometric circumstances are fulfilled. According to Wyllie and Mah [34] Plane failure develops with the following circumstances: (a) the strike of the joint planes (α_j) on the sliding has a strike orientation parallel within ± 20° to the slope strike (α_s); (b) the dip of joint plane must be less than the slope angle or $\beta_s > \beta_j$; (c) the dip of the joint should be greater than the friction angle or $\beta_j > \Phi$; and (d) the upper part of the sliding surface must either intersect the upper slope or terminate in a tension crack (see Fig. 3). The factor of safety for plane failure is computed by completing all forces works on the slope into components parallel and normal to the sliding plane; yet, this research does not calculate the factor of safety.

3.1.2 Wedge Failure

Wedge failures can happen in wider range of geologic structure and geometric circumstances compare to plane failures; the study of wedge failure is significantly important in rock slope engineering researches [34]. The stereography projection, this research able to defines the orientation of the line of intersection (trend), the direction of sliding (plunge), and the shape of the wedge. This information can utilize to study the potential wedge failure on the slope face.

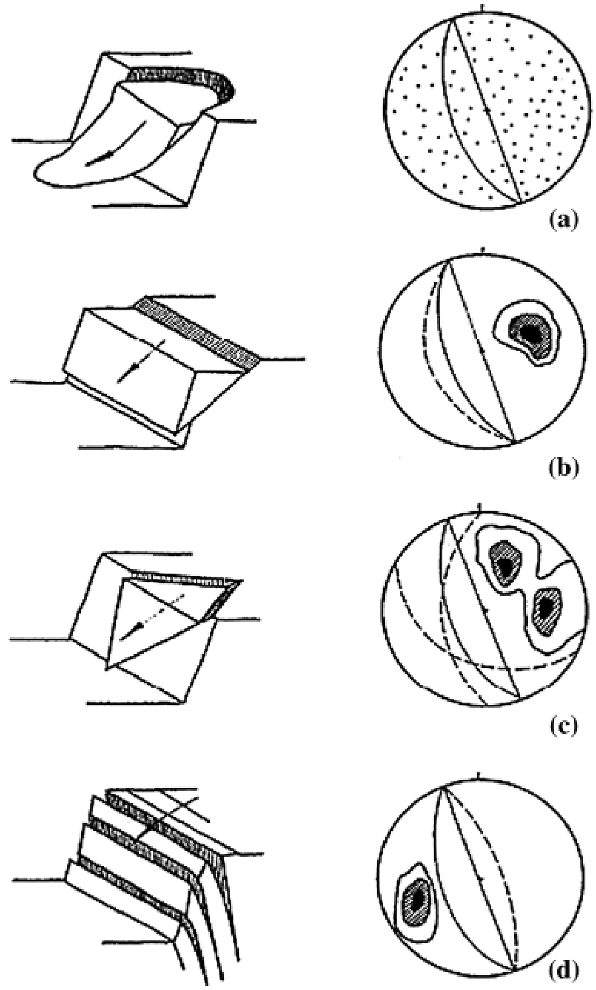

Figure 2: Geometric condition for rock slope failures (left) and Stereography pattern of rock slope failures (right); (a) rotational failure, (b) planar failure, (c) Wedge failure, (d) toppling failure [17]

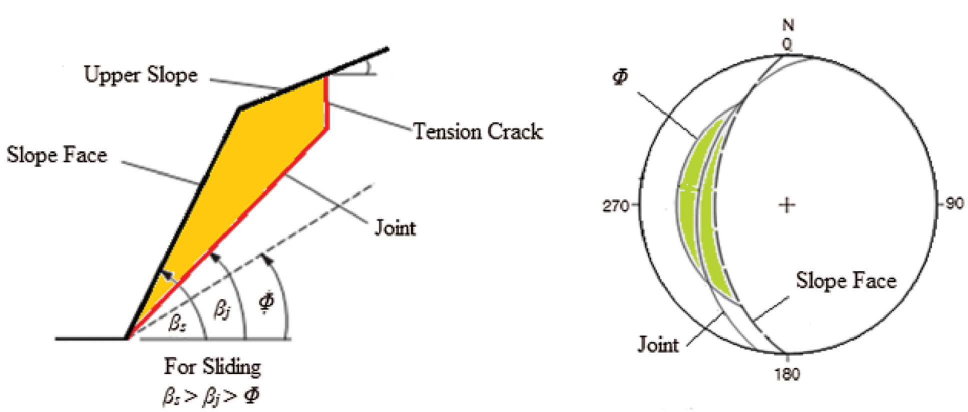

Figure 3: Geometric circumstances for Plane failure, (a) Pictorial view of wedge failure, (b) Stereography projection, after modified from Wyllie & Mah [34]

According to Wyllie & Mah [34], the wedge failure develops if two intersection joints meet inside the slope and form a wedge-block. The plunge (β_i), as the angle of two intersections relatively meet horizontally, must also be flatter than the slope angle (β_s) but higher than the friction angle (Φ) of the two slide planes, or $\beta_s > \beta_i > \Phi$; and the plunge direction should be out of the slope face for sliding to be feasible (see Fig. 4).

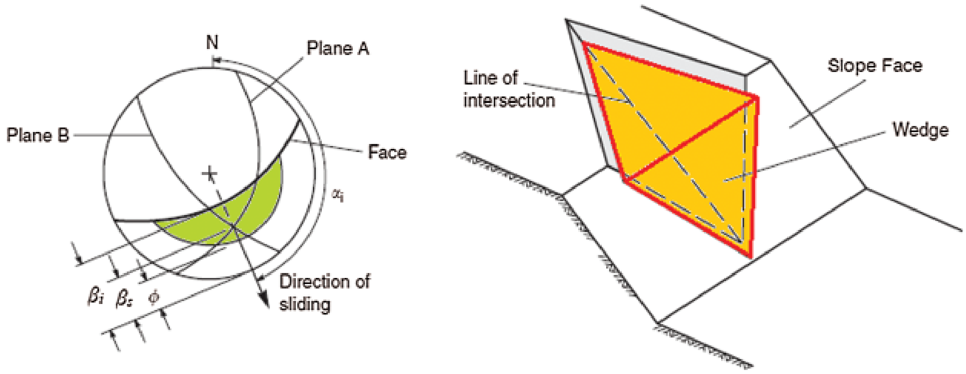

Figure 4: Geometric circumstances for wedge failure (a) stereography projection showing the orientation of the line of intersection, and the range of the plunge of the line of intersection (β_s) where failure is feasible, (b) pictorial view of wedge failure after modified from Wyllie & Mah [34]

3.1.3 Toppling Failure

Wyllie & Mah [34] stated that, the toppling slope failure interfere by the rotation of blocks or columns of rock on the slope. A like to plane and wedge failures, the stability analysis of toppling failures beginning by conducting a kinematic analysis of the structural geology in stereography projection to identify potential toppling circumstance.

It has various types such as; flexural, block-flexure, block, and secondary toppling modes [34]. The toppling rock failure happens when the strike joints (α_j) opposite slope face (α_s). Rotational failure often occurs when the rock has a high frequency of the joint as well as closely joint, accordingly the high weathering put a rock mass close to the residual soil.

3.2 Rock Mass Rating (RMR)

The Council of Scientific and Industrial Research (CSIR) in South Africa developed RMR, and Bieniawski introduced it in 1973. The RMR rock mass system had undergone multiple modifications in 1974, 1975, 1979, 1984, and 1989 [31]. RMR was mainly developed based on the historical case of the civil engineering project, and the last RMR 1989 was the most suitable classification for mining and civil engineering works concerning rock engineering [16]. Bieniawski [8] proposed several parameters to evaluate rock quality, including the strength of intact rock, Rock Quality Designation (RQD), number of spacing, joints condition, and water condition. RMR is widely used in engineering rock mass classification in Indonesia for civil or mining applications.

RMR has many advantages, including its ability to compare rock quality in site both on surface and underground project, ease of application, it applicable to use in empirical approaches including the Hoek and Brown failure criteria. In additional, RMR classification is commonly used as a communication bridging among geologist, civil engineer, and non-technical staff. The RMR parameters denoted in Tab. 2 classify the geologic structure, joint, and water condition into a different rating to compute the total

Table 1: Guidelines for classification of joint conditions [8]

Persistence	<1 m	1–3 m	3–10 m	10–20 m	>20 m
Rating	6	4	2	1	0
Aperture	None	<0.1 mm	0.1–1.0 mm	1–5 mm	>5 mm
Rating	6	5	4	1	0
Roughness	Very rough	Rough	Slightly rough	Smooth	Slickenside
Rating	6	5	3	1	0
Infilling	None	Hard Filling <5 mm	Hard Filling >5 mm	Soft Filling <5 mm	Soft Filling >5 mm
Rating	6	4	2	2	0
Weathering	Unweathered	Slightly weathered	Moderately weathered	Highly weathered	Decomposed
Rating	6	5	3	1	0

number of RMR. The scores are presented in a range to dismiss subjective interpretations among investigators.

3.2.1 *Strength of Intact Rock Material*

The strength of the intact rock is obtained from rock sample taken from the slopes. In RMR, the strength of intact rocks is based on UCS (uniaxial compressive strength), point load strength, empirical equation between V_{PL} and UCS developed by Nourani et al. [22]; yet this study employ field estimation UCS from geological hammer.

3.2.2 *Rock Quality Designation (RQD)*

RQD introduced by Deere [10] as a tool for assessing rock quality in rock engineering practices. The RQD value based on the percent core-recovery which calculate only length of core more than 100 mm (4 inch.) divided by the total length of core [10]. For slope, The RQD score was computed by applying a correlation equation of the volumetric joint (*Jv*) on the slope as proposed by Palmstrom [23], denoted in Eq. (1). *Jv* itself described a volumetric of discontinuity frequency that is similar to the number of discontinuities in 1 m^3 calculated using Eq. (2), the illustration of *Jv* as show in Fig. 5. The *S* in Eq. (2) refers to the spacing of joint sets.

$$RQD = 110 - 2.5\,Jv \tag{1}$$

$$Jv = 1/S_1 + 1/S_2 + 1/S_3 + \ldots + 1/S_n \tag{2}$$

3.2.3 *Joint or Discontinuity Spacing*

In rock engineering, the term discontinuity including beddings, joints, foliations, mayor or minor faults, shear zones, or other surfaces fractures. The perpendicular distance between two discontinuities namely as discontinuity spacing, accordingly it should be measured for all sets of discontinuities [32].

Table 2: Rock Mass Rating system after Bieniawski [8]

	Parameters		Range of values				
1	Strength of Intact Rock Material	*Point Load Strength Index*	>10 MPa	4–10 MPa	2–4 MPa	1–2 MPa	For this low range, UCS test is preferred
		Uniaxial Compressive Strength (UCS)	>250 MPa	100–250 MPa	50–100 MPa	25–50 MPa	5–25 MPa 1–5 MPa <1 MPa
	Rating		15	12	7	4	2 1 0
2	Rock Quality Designation (RQD)		90–100%	75–90%	50–75%	25–50%	<25%
	Rating		20	17	13	8	3
3	Spacing of Discontinuities		>2 m	0, 6–2 m	200–600 mm	60–200 mm	<60 mm
	Rating		20	15	10	8	0
4	Condition of Discontinuities		Very rough surfaces, not continuous No separation Unweathered wall rock	Slightly rough surfaces Separation <1 mm Slightly weathered walls	Slightly rough surfaces Separation <1 mm Highly weathered walls	Slicken sided surfaces or gouge <5 mm thick or separation 1–5 mm Continuous	Soft gouge >5 mm thick or separation >5 mm Continuous
	Rating		30	25	20	10	0
5	Ground Water	Inflow per 10 m tunnel length (l/m)	0	<10	10–25	25–125	>125
		(Joint water press)/(Major principal σ)	0	<0,1	0,1–0,2	0,2–0,5	>0,5
		General conditions	Completely dry	Damp	Wet	Dripping	Flowing
	Rating		15	10	7	4	0

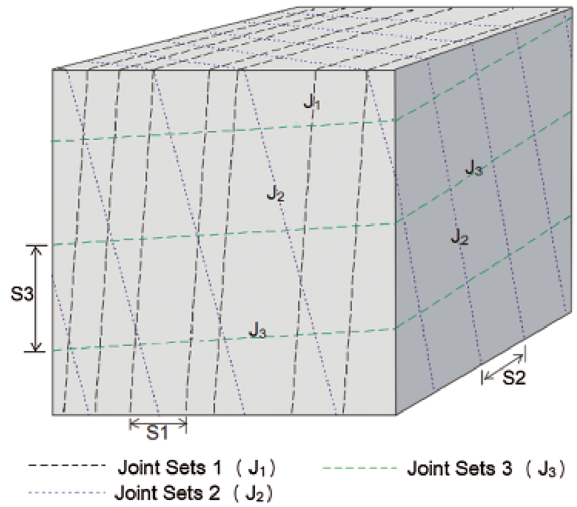

Figure 5: Joint Sets and the Joint Sets spacing (*S*) in 3D after modified from Palmstrom [23]

3.2.4 Joint Condition

Joint condition parameters include roughness of discontinuity surfaces, aperture (separation), persistence (length or continuity), degree of weathering of rock wall or the planes, and infilling material. The rating each parameters as noted in Tab. 1.

3.2.5 Groundwater Condition

The groundwater condition or water pressure will affect the shear strength of discontinuity plane. RMR classification commonly used in tunnels and slope; In the case of tunnels, the rate of inflow of groundwater should be determined in litres per minute at every 10 m length of the tunnel. The similar method applied when it study on slope, groundwater condition practically described as completely dry, damp, wet, dripping, and flowing [31]. The groundwater condition rating as denoted in Tab. 2.

3.3 Slope Mass Rating (SMR)

Romana [26] developed SMR by adjusting the Bieniawski's RMR system to make the classification reliable for slope analysis. The SMR considers the correlation between the dip angle and the strike of slope face as well as the dip and strike of discontinuity plane (joints) on the slope. Romana [26] proposed the following equations (Eqs. (3)–(5)).

$$SMR \quad = RMR_b + (F_1.F_2.F_3) + F_4 \tag{3}$$

$$F_1 = \left[1 - Sin\left(\alpha_s - \alpha_j\right)\right]^2 \tag{4}$$

$$F_2 = Tan\ \beta_j \tag{5}$$

F_1, F_2, F_3, and F_4 are the added value as the adjustment factors related to slope and joints orientation, while $\alpha_{s,}$ $\alpha_{j,}$ and β_j are the slope strike, the joint strike, and the joint dips respectively. F_1 rating, computed by applying Eq. (4), explains the parallelism between the joints and slopes strike. F_2, calculated using Eq. (5), refers to a connection between the slope face angle and the joint dips. Hence, F_3 explains the relationship between the slope angle β_s and the joint dips β_j, and the value mainly depends on the type of the failure. Planar and toppling slope failures are commonly used in SMR analysis [6]. However, this research considered the wedge failure, added by Anbalagan et al. [2], to Romana's SMR. F_4 respects to the adjustment of the excavation method as presented in Tab. 3. A study employing both RMR and SMR rock mass classifications to investigate the slope stability in Aceh Province has been conducted by Rusydy et al. [27]. More detail the adjustment factor for each type of failure as denoted in Tab. 3 and adjustment factor F_4 in Tab. 4.

Table 3: Adjustment factors for different type of failures [26]

Case of Slope Failure		Very Favourable	Favourable	Fair	Unfavourable	Very Unfavourable
P	$\|\alpha_j - \alpha_s\|$	>30°	30°–20°	20°–10°	10°–5°	<5°
T	$\|\alpha_j - \alpha_s - 180°\|$					
W	$\|\alpha_i - \alpha_s\|$					
P/T/W	$\mathbf{F_1}$	0.15	0.40	0.70	0.85	1.00
P	$\|\beta_j\|$	<20°	20°–30°	30°–35°	35°–45°	>45°
W	$\|\beta_i\|$					
P/W	$\mathbf{F_2}$	0.15	0.40	0.70	0.85	1.00
T	$\mathbf{F_2}$	1.00	1.00	1.00	1.00	1.00
P	$\|\beta_j - \beta_s\|$	>10°	10°–0°	0°	0°–(−10°)	<−10°
W	$\|\beta_i - \beta_s\|$					
T	$\|\beta_j + \beta_s\|$	<110°	110°–120°	>120°	–	–
P/W/T	$\mathbf{F_3}$	0	−6	−25	−50	−60

Table 4: The adjustment factor F_4 [26]

Excavation Method	F_4 Value
Natural slope	15
Pre-splitting	10
Smooth blasting	8
Normal blasting or mechanical excavation	0
Deficient blasting	−8

4 Results and Discussion

This study has been conducted on six rock slopes for rock slope kinematic analysis, rock mass rating (RMR), and slope mass rating (SMR). The field photographs of investigated slopes have been illustrated in Fig. 6 and detailed discussion over stability assessment has been provided in further sections. The rock lithology found in study areas is tilted argillaceous limestone with thin bedding and blocky. The structural geology feature entangles rock slopes stability in USAID highway.

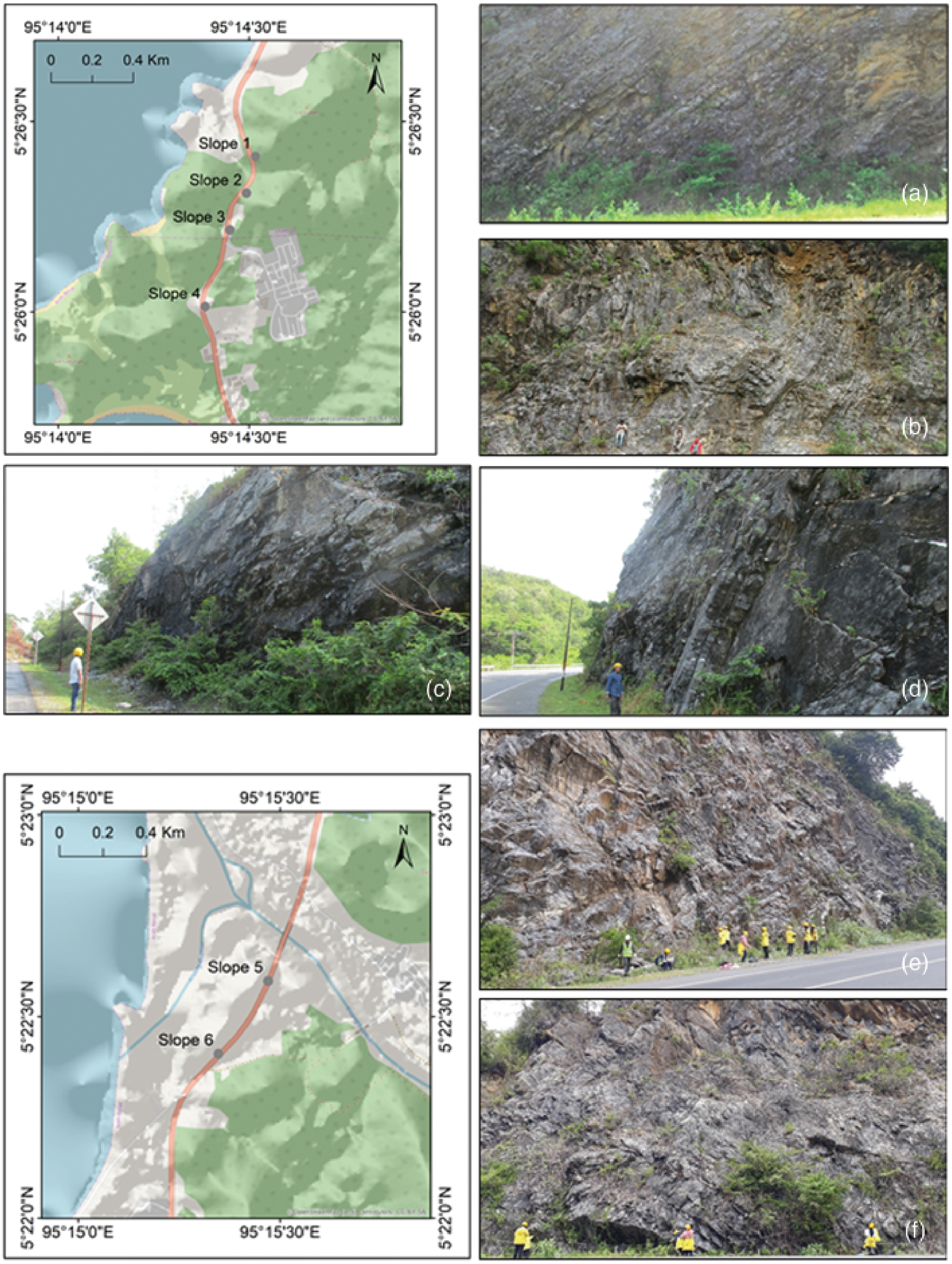

Figure 6: Field Photographs of rock slopes along USAID highway, (a) Slope 1, (b) Slope 2, (c) Slope 3, (d) Slope 4, (e) Slope 5, and (f) Slope 6

4.1 Rock Kinematic Analysis

First investigation performed in Slope 1, it reveals that the intersection between J_1 and J_2 form the wedge-shaped block, the trend (α_i) of this intersection in almost same direction of slope face. The joint sets J_3 develop planar failure due to is parallelism to slope face, the strike of J_3 (α_j) is N 158° E while the strike of slope (α_s) is N 160° E, it only different 2° as shown in Fig. 7b and Tab. 5. Kinematic analysis

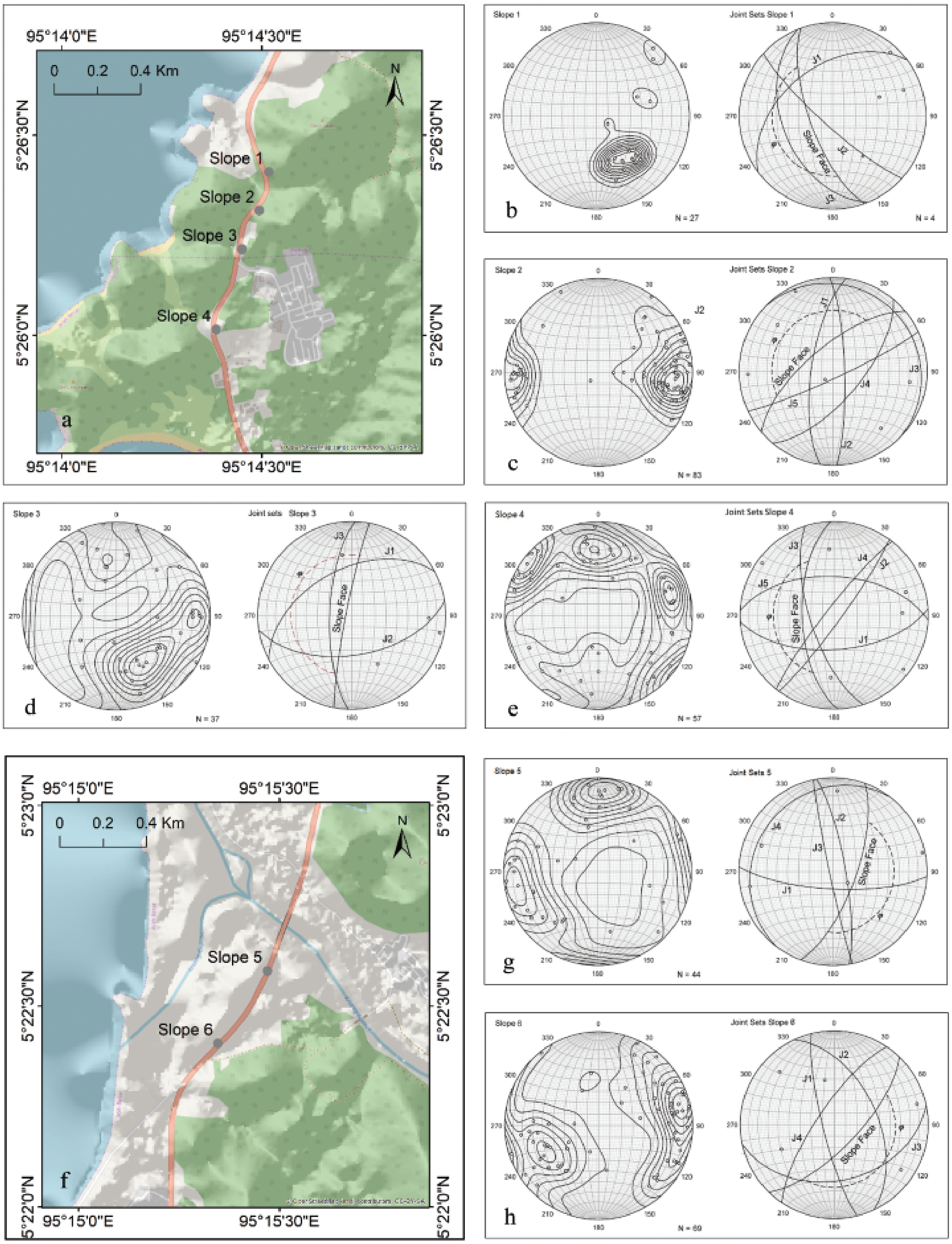

Figure 7: The location of the investigated slopes following by stereography plot for rock kinematic analysis. (a) Zone A, (b) Slope 1, (c) Slope 2, (d) Slope 3, (e) Slope 5, (f) Zone B, (g) Slope 6, and (h) Slope 7

Table 5: Rock slope geometric and *Joint Set* along USAID highway from 17 to 26 Km

Slopes	Joint Sets	Joint Orientation (α_j/β_j)	Joint Numbers	Basic Friction Angle (Φ)	Slope Orientation (α_s/β_s)	Type of Failures and Joint Sets Involved
Slope 1	J_1	233°/45°	23	35°	160°/70°	Plane and Wedge
5.439634° N	J_2	132°/81°	2			
95.242266° E	J_3	158°/45°	2			
Slope 2	J_1	188°/71°	62	25°	230°/68°	Toppling
5.438658° N	J_2	358°/80°	18			
95.241803° E	J_3	314°/10°	1			
	J_4	39°/66°	1			
	J_5	65°/84°	1			
Slope 3	J_1	242°/49°	18	30°	191°/85°	Plane
5.436811° N	J_2	81°/55°	11			
95.240970° E	J_3	182°/71°	8			
Slope 4	J_1	86°/60°	15	30°	178°/62°	Plane
5.433893° N	J_2	36°/84°	14			
95.239886° E	J_3	162°/69°	12			
	J_4	218°/83°	8			
	J_5	273°/56°	8			
Slope 5	J_1	93°/75°	17	28°	20°/70°	Toppling
5.376463° N	J_2	350°/79°	18			
95.257759° E	J_3	168°/87°	3			
	J_4	217°/16°	6			
Slope 6	J_1	166°/77°	32	27°	44°/70°	Wedge & Toppling
5.373618° N	J_2	335°/52°	26			
95.255989° E	J_3	78°/40°	2			
	J_4	214°/75°	9			

conclude that Wedge and planar slope failures possible to be occurred in Slope 1 due to the intersection amid those joint sets inside or higher than basic friction angle (Φ) yet it less than slope angle (β_s).

Slope kinematic analysis in Slope 2 indicate that, the intersection between J_1 and J_2 trigger the wedge-block failure, yet the plunge angle (β_i) develop among those joints set lower than basic friction angle (Φ), it mean the Slope 2 is secure from wedge slope failure. The circumstances occur to J_1 and J_2 in Slope 3, the plunge angle develop lower than basic friction, accordingly Slope 3 safe from wedge failure. Joint J_4 and J_5 in Slope 2, has an opposite orientation to the slope face, it would trigger toppling failure as shown in Fig. 7c.

The planar failure likely occur in Slope 3 due to joint set J_3 parallel to slope face about 9° whereas the strike of slope (α_s) is N 191° E and the strike (α_j) of J_3 is N 182° E. In other hand, the dip of J_3 is higher (β_j = 71°) than basic friction angle (Φ = 30°) but less than slope angle (β_s = 85°). All the conditions for planar failure as noted by Wyllie & Mah [34] are met in Slope 3 except a tension cracks on top of the slope. This study was unable to investigate the tension crack on of slope due to insufficient equipment. In spite of that, three requirement are found in Slope 3 and it enough to develop planar failure in Slope 3. In Slope 5, this study find five joint sets and the joint numbers distribution each joint set are almost similar as shown in Tab. 5. The stereography and slope kinematic analysis as illustrated in Fig. 7e concluded only planar failure possible to be occurred in Slope 5 and it similar to Slope 3.

In Slope 4, this study reveal five joint sets and data distribution each joint set are almost similar as shown in Tab. 5. The stereography and slope kinematic analysis as illustrated in Fig. 7e concluded only planar failure possible to be occurred in Slope 4 and it similar to Slope 3. Joint sets J_3 responsible for planar failure, it has strike of joint (α_j) N 162° E while α_s is N 178° E the different only 16° or less than 20°. Another condition put planar failure likely occur in Slope 5 is the dip of joint (β_j = 69°) higher than basic friction angle (Φ = 30°), but lower than slope angle (β_s = 70°).

Slope 5 and Slope 6 situate 7 Km from previous slope, in Fig. 1 it illustrate as zone B (for more detail see Fig. 7f). Slope 5 and 6 had four joint which would trigger the wedge and toppling failures in Slope 7 and toppling in Slope 6 as shown in Figs. 6h and 7g. The toppling failure in Slope 5 and Slope 6 responsible by joint sets J_4 Slope 6 and J_4 Slope 6 which only had six joints on the Slope 5 and nine joints in Slope 6. The wedge-block formed by joints intersection between J_2 and J_5. The plunge develop is 32° while the basic friction angle is 27°; accordingly the wedge failure possibly to be occurred in Slope 6.

4.2 Rock Mass Rating (RMR)

The RMR parameters utilize to compute the total number of RMR as show Tab. 2, the joints condition in Tab. 1. The scores RMR in Tab. 2 are presented in a range to dismiss subjective interpretations during interpretation. The first parameter is strength of intact rock reveal from field estimation using geological hammer; accordingly, the results of UCS are in range of 25 to 50 Mpa; resulting in the rate of 4 points of the strength of intact rock. The RQD value computed using Palmstrom [23] equation shows that all slopes have 100% value of RQD. The *Jv* number in all slopes ranging from 2.7 to 4 with true discontinuity spacing between 0.28 and 0.37 meters contributes to the high value. Most of joints in those slopes are developed as rock bedding, random fractures among bedding, and micro faults. The field investigation reveals that the bedding thickness is between 0.2 and 0.5 meters.

The joints condition consists of five parameters. The condition and the rating of each parameter for each joint sets can be seen in Tab. 5. The joints condition of the rock slopes exposed in the field is similar for its roughness, yet it is slightly different in term of the persistence, apertures, filling materials, and weathering degree. Overall, the rating of joints condition on those slopes ranges from 8 to 18, as denoted in Tab. 6. In term of the groundwater condition, all the slopes have dry to damp condition. The results of groundwater rating can be seen in Tab. 7.

This study used J_1 condition to calculate the total RMR value by considering the huge joints number of J_1, resulting in the rating value of joints condition of 12, 11, 13, 15, 13, and 13 for slope 1 to 6 respectively. The total number of RMR_{basic} for each slope does not show any significant difference; the rock quality rating ranges from Good Rock to Fair Rock, as presented in Tab. 5. The rating is slightly different for those slopes, but it is classified as the different rock mass quality based on RMR classification developed by Bieniawski [8]. The Good Rock ranges from 61 to 80, and Fair Rock is 41–60; however, the RMR rating among those slopes are slightly different. Historically, the rocks in those slopes were formed simultaneously in the latest Jurassic to early Cretaceous resulting in the similar lithology. In 2007, all those slopes were excavated using

Table 6: The rock joints condition along the 17th to 26th Km USAID Highway in Aceh province

Slopes and Lithology	Joint Sets	Cond.. and rating	Joints Condition Parameters					Rating of Joint Cond..
			Persistence	Aperture	Roughness [9]	Filling	Weathering [9]	
Slope 1 Argillaceous Limestone	J1	Cond..	3–10 m	>5 mm	Rough	soft >5 mm	Slightly	12
		Rating	2	0	5	0	5	
	J2	Cond..	3–10 m	>5 mm	Rough	soft >5 mm	Moderate	10
		Rating	2	0	5	0	3	
	J3	Cond..	3–10 m	>5 mm	Rough	soft >5 mm	Moderate	10
		Rating	2	0	5	0	3	
Slope 2 Argillaceous Limestone	J1	Cond..	10–20 m	>5 mm	Rough	soft >5 mm	Moderate-Slightly	11
		Rating	1	0	5	1	4	
	J2	Cond..	3–10 m	0,1-1 mm	Rough	soft <5 mm	Moderate	15
		Rating	2	3	5	2	3	
	J3	Cond..	10–20 m	1–5 mm	Rough	soft <5 mm	Highly	10
		Rating	1	1	5	2	1	
	J4	Cond..	3–10 m	>5 mm	Rough	soft >5 mm	Highly	8
		Rating	2	0	5	0	1	
	J5	Cond..	3–10 m	>5 mm	Rough	soft >5 mm	Slightly	12
		Rating	2	0	5	0	5	
Slope 3 Argillaceous Limestone	J1	Cond..	3–10 m	1–5 mm	Rough	soft <5 mm	Moderate	13
		Rating	2	1	5	2	3	
	J2	Cond..	1–3 m	1–5 mm	Rough	soft <5 mm	Moderate-Slightly	16
		Rating	4	1	5	2	4	
	J3	Cond..	1–3 m	1–5 mm	Rough	soft <5 mm	Moderate	15
		Rating	4	1	5	2	3	

(Continued)

Table 6 (continued).

Slopes and Lithology	Joint Sets	Cond.. and rating	Joints Condition Parameters					Rating of Joint Cond..
			Persistence	Aperture	Roughness [9]	Filling	Weathering [9]	
Slope 4 Argillaceous Limestone	J1	Cond..	1–3 m	1–5 mm	Rough	soft <5 mm	Moderate	15
		Rating	4	1	5	2	3	
	J2	Cond..	1–3 m	1–5 mm	Slightly rough	soft <5 mm	Slightly	15
		Rating	4	1	3	2	5	
	J3	Cond..	3–10 m	>5 mm	Rough	soft >5 mm	Slightly	12
		Rating	2	0	5	0	5	
	J4	Cond..	3–10 m	0,1-1 mm	Rough	soft <5 mm	Slightly	17
		Rating	2	3	5	2	5	
	J5	Cond..	1–3 m	0,1-1 mm	Rough	soft <5 mm	Moderate-Slightly	18
		Rating	4	3	5	2	4	
Slope 5 Argillaceous Limestone	J1	Cond..	1–3 m	>5 mm	Rough	soft <5 mm	Moderate	14
		Rating	4	0	5	2	3	
	J2	Cond..	1–3 m	1–5 mm	Rough	soft <5 mm	Moderate	13
		Rating	4	1	5	2	3	
	J3	Cond..	1–3 m	>5 mm	Very rough	soft >5 mm	Moderate	13
		Rating	4	0	6	0	3	
	J4	Cond..	1–3 m	1–5 mm	Rough	Hard <5 mm	Moderate	17
		Rating	4	1	5	4	3	

Table 6 (continued).

Slopes and Lithology	Joint Sets	Cond.. and rating	Joints Condition Parameters					Rating of Joint Cond..
			Persistence	Aperture	Roughness [9]	Filling	Weathering [9]	
Slope 6 Argillaceous Limestone	J1	Cond..	3–10 m	1–5 mm	Rough	soft <5 mm	Moderate	13
		Rating	2	1	5	2	3	
	J2	Cond..	1–3 m	4 mm	Rough	soft <5 mm	Moderate	16
		Rating	4	2	5	2	3	
	J3	Cond..	1–3 m	1–5 mm	Rough	Hard <5 mm	Moderate	17
		Rating	4	1	5	4	3	
	J4	Cond..	1–3 m	1–5 mm	Rough	Hard 5 mm	Moderate	16
		Rating	4	1	5	3	3	

Table 7: RMR rating of each slope along the 17th to 26th Km USAID Highway

No.	RMR Parameters	Slope 1	Slope 2	Slope 3	Slope 4	Slope 5	Slope 6
1.	Strength of Intact Rock	25–50 MPa	25–50 MPa	25–50 MPa	25–50 MPa	25–50 MPa	25–50 MPa
	Rating	*4*	*4*	*4*	*4*	*4*	*4*
2.	RQD	100%	100%	100%	100%	100%	100%
	Rating	*20*	*20*	*20*	*20*	*20*	*20*
3.	Spacing of Discontinuities	0.25 m	0.37 m	0.44 m	0.28 m	0.32	0.36
	Rating	*10*	*10*	*10*	*10*	*10*	*10*
4.	Condition of Discontinuities	See Tab. 6 (J1)	See Tab. 6 (J1)	See Tab. 6 (J1)	See Tab. 6 (J1)	See Tab. 6 (J2)	See Tab. 6 (J1)
	Rating	*12*	*11*	*13*	*15*	*13*	*13*
5.	Groundwater Condition	Dry to Damp	Dry to Damp	Dry to Damp	Dry	Dry	Dry
	Rating	*12*	*12*	*12*	*15*	*15*	*15*
RMR$_b$		***58***	***57***	***59***	***64***	***62***	***62***
Quality of Rock Mass		***Fair Rock***	***Fair Rock***	***Fair Rock***	***Good Rock***	***Good Rock***	***Good Rock***

normal blasting and mechanical equipment; consequently, those slopes were exposed to the atmosphere at the same time. The similar period of forming, exposing, and rock lithology lead to those slopes having slightly mutual joint surface conditions and rock structures. Thus, all slopes have equal rock mass quality.

4.3 Slope Mass Rating (SMR)

Slope kinematic analysis reveals that wedge and planar slope failure are possible to occur at Slope 1 and 6, toppling failures at Slope 2 and 5, and planar failure at Slope 3 and 4. The SMR was computed by applying Eq. (3), while the adjustment factor was calculated by Eqs. (4) and (5) together with the standard value for the excavation method, as shown in Tab. 4. RMR_b is used to compute SMR of each slope as presented in Tab. 7, indicating that the SMR analyses require RMR_b and kinematic analysis results. This research combine both methods to calculate the final SMR presented in Tab. 8.

Table 8: SMR rating of each slope along the 17th to 26th km of USAID Highway and the rock failure probability

Locations	*Joints Set involved*	*Type of Failures from Kinematic Analysis*	*RMR_b*	*F1*	*F2*	*F3*	*F4*	*SMR*	*Probability of Failure* [26]
Slope 1	J_1 and J_2	Wedge	58	0.15	0.84	−60	0	50	40%
	J_3	Planar	58	0.93	1	−60	0	3	90%
Slope 2	J_4	Toppling	57	0.15	1	−25	0	53	40%
	J_5	Toppling	57	1	1	−25	0	32	60%
Slope 3	J_3	Planar	59	0.71	1	−60	0	16	90%
Slope 4	J_3	Planar	64	0.52	1	−25	0	51	40%
Slope 5	J_3	Toppling	62	0.22	1	0	0	62	20%
	J_4	Toppling	62	0.50	1	−60	0	32	60%
Slope 6	J_2 and J_3	Wedge	62	0.71	0.65	−60	0	34	60%
	J_4	Toppling	62	0.68	1	0	0	62	20%

The wedge failures occur in two slopes because of the interaction between J_1 and J_2 in Slope 1 and J_2 and J_3 in Slope 6. The SMR rating for both slopes is 50 and 34, according to Romana [26] these rating will result in the slope probability of 40% and 60%. Planar failure is likely occur in Slope 1, 3, and 4; the kinematic analysis leads to the slope faces being parallel to joint dip direction at less than 20°. Slope 1 and 3 have the highest probability of planar failure, up to 90%, whilst it is 40% for Slope 4. Slope 2, 5, and 6 experience toppling failure, with 20%–60% of failure probability in all joint sets.

The RMR rating for all slopes is almost similar. However, the SMR rating varies and depends on the orientation of the joint sets and the slope, especially the connection between the slope angle β_s and the joint dips β_j represented by F_3. The value of F_3 ranges from 0 (very favourable) to −60 (very unfavourable). The unfavourable condition occurs if the $\beta_j - \beta_s$ is less than −10°, such as the planar failure in Slope 1 with 58 RMR and 3 SMR; and in Slope 3 with 59 RMR and 16 SMR.

5 Conclusions

The results obtained by kinematic analysis performed indicate that three types of failures (planar, toppling and wedge failure) are possible. Planar failure may occur in Slope 1, 3, and 4, while wedge failure may happen in Slope 1 and 6, and toppling failure is likely to occur in Slope 2, 5, and 6. The adverse orientation of joints with respect to slope, slope geometry, and basic friction angle depending on the roughness of joints are contributing to the failures.

The rock mass rating (RMR) in the investigated slopes seem to be mutual. The slopes studied have similar RMR because of the corresponding similar lithological and geotechnical characteristics. However, the similarity of RMR or quality does not correspond with SMR and its stabilities. This differentiate influenced by the connection between the slope angle βs and the joint dips βj on the slope which represented by F3 adjustment factor. Slope 1 and 3 had 90% probabilities of planar failure, accordingly those slopes required more analysis to determine the factor of safety.

For future research, we suggest employing an integrated methods, including terrestrial laser scanning method and photogrammetric approach to study the whole slope kinematic analysis. Concerning the rock mass classification, we recommend conducting other rock mass classification such, geological strength index (GSI), Q-system, and seismic refraction tomography to determine the correlation among those rock mass classification with pressure wave velocity (V_{PF}). In term of the rock slope stability, the finite element method to determine the factor of safety (FoS) should perform in those slopes by adopting the Hoek and Brown failure criteria in future.

Acknowledgement: Authors would like to express profound gratitude to *Lembaga Penelitian dan Pengabdian Kepada Masyarakat* Universitas Syiah Kuala for providing research grant through *Penelitian Lektor* scheme 2019 and to Geology Engineering and Mining Engineering students for supporting this research during the data collection and field trips.

References

1. Alejano, L. R., Muralha, J., Ulusay, R., Li, C. C., Pérez-Rey, I. et al. (2018). ISRM suggested method for determining the basic friction angle of planar rock surfaces by means of tilt tests. *Rock Mechanics and Rock Engineering, 51(12),* 3853–3859. DOI 10.1007/s00603-018-1627-6.
2. Anbalagan, R., Sharma, S., Raghuvanshi, T. K. (1992). Rock mass stability evaluation using modified SMR approach. the 6th National Symposium on Rock Mechanics. *Proceeding of the 6th National Symposium on Rock Mechanics*, 258–268.
3. Barber, A. J. (2000). The origin of the Woyla Terranes in Sumatra and the Late Mesozoic evolution of the Sundaland margin. *Journal of Asian Earth Science, 18(6),* 713–738. DOI 10.1016/S1367-9120(00)00024-9.
4. Barber, A. J., Crow, M. J. (2005). Pre-tertiary stratigraphy. In: Barber, A. J., Crow, M. J., Milson, J. S., (eds.) *Sumatra: Geology, Resources, and Tectonic Evolution*. London: Geological Society, 41.
5. Barton, N. R., Lien, R., Lunde, J. (1974). Engineering classification of rock masses for the design of tunnel support. *Rock Mechanics, 6(4),* 189–236. DOI 10.1007/BF01239496.
6. Basahel, H., Mitri, H. (2017). Application of rock mass classification systems to rock slope stability assessment: a case study. *Journal of Rock Mechanics and Geotechnical Engineering, 9(6),* 993–1009. DOI 10.1016/j.jrmge.2017.07.007.
7. Bennet, J. D., Bridge, D. M., Cameron, D. R., Djunuddin, A., Ghazali, S. A., et al. (1981). *Geologic 1: 250,000 Map of Banda Aceh Quadragle, Sumatra*. Bandung: Geological Research and Development Centar (GRDC).
8. Bieniawski, Z. T. (1989). *Engineering Rock Mass Classification*. New York: John Wiley & Sons.
9. Brown, E. T. (1981). *Rock Characterization, Testing and Monitoring, ISRM Suggested Methods. (E. T. Brown, Ed.)*. Oxford: Published for the Commission on Testing Methods, International Society for Rock Mechanics by Pergamon Press.
10. Deere, D. U. (1968). Geological considerations. In: Ambraseys, N., (ed.) *Rock Mechanics in Engineering Practice*. London: John Wiley, 1–20.
11. Fernández-Blanco, D., Philippon, M., Hagke, C. V. (2016). Structure and kinematics of the Sumatran fault system in North Sumatra (Indonesia). *Tectonophysics, 693,* 453–464. DOI 10.1016/j.tecto.2016.04.050.
12. Ghani, R. A., Goh, T. L., Hariri, A. M., Baizura, Y. N. (2011). Field and laboratory-based approach for the determination of friction angle of geological discontinuities of Malaysian granites. *ASEAN Journal on Science and Technology for Development, 28(2),* 151–155. DOI 10.29037/ajstd.41.

13. Goodman, R. E. (1989). *Introduction to Rock Mechanics,* 2nd edition. New York: Wiley.
14. Grelle, G., Revellino, P., Donnarumma, A., Guadagno, F. M. (2011). Bedding control on landslides: a methodological approach for computer-aided mapping analysis. *Natural Hazards and Earth System Science, 11(5),* 1395–1409. DOI 10.5194/nhess-11-1395-2011.
15. Gurocak, Z., Alemdag, S., Zaman, M. M. (2008). Rock slope stability and excavatability assessment of rocks at the Kapikaya dam site, Turkey. *Engineering Geology, 96(1–2),* 17–27. DOI 10.1016/j.enggeo.2007.08.005.
16. Hoek, E. (2007). Practical Rock Engineering. 1st edition. Canada: Rock ScienceRetrieved July 5, 2016. Available at https://www.rocscience.com/documents/hoek/corner/Practical-Rock-Engineering-Full-Text.pdf.
17. Hoek, E., Bray, J. W. (1981). *Rock Slope Engineering*. 3rd edition. London: Institute of Mining and Metallurgy.
18. Hoek, E., Brown, E. T. (1997). Practical estimates of rock mass strength. *International Journal of Rock Mechanics and Mining Sciences, 34(8),* 1165–1186. DOI 10.1016/S1365-1609(97)80069-X.
19. Lee, C. Y., Wang, I. T. (2011). *Analysis of Highway Slope Failure by an Application of the Stereographic Projection*. Taiwan: World Academy of Science, Engineering and Technology.
20. McCaffrey, R. (2009). The tectonic framework of the Sumatran subduction zone. *Annual Review of Earth and Planetary Sciences, 37(1),* 345–366. DOI 10.1146/annurev.earth.031208.100212.
21. Muksin, U., Rusydy, I., Erbas, K., Ismail, N. (2018). Investigation of Aceh Segment and Seulimeum Fault by using seismological data; a preliminary result. *Journal of Physics: Conference Series*, IOP Publishing. *Vol. 1011,* 012031.
22. Nourani, M. H., Moghadder, M. T., Safari, M. (2017). Classification and assessment of rock mass parameters in Choghart iron mine using P-wave velocity. *Journal of Rock Mechanics and Geotechnical Engineering, 9(2),* 318–328. DOI 10.1016/j.jrmge.2016.11.006.
23. Palmstrom, A. (2005). Measurements of and correlations between block size and rock quality designation (RQD). *Tunnelling and Underground Space Technology, 20(4),* 362–377. DOI 10.1016/j.tust.2005.01.005.
24. Pantelidis, L. (2009). Rock slope stability assessment through rock mass classification systems. *International Journal of Rock Mechanics and Mining Sciences, 46(2),* 315–325. DOI 10.1016/j.ijrmms.2008.06.003.
25. Rai, M. A., Kramadibrata, S., Wattimena, R. K. (2014). *Mekanika Batuan*. Bandung: Penerbit ITB.
26. Romana, M. (1985). New adjustment ratings for application of Bieniawski classification to slope. *Proceedings of the International Symposium on the Role of Rock Mechanics in Excavations for Mining and Civil Works* , Mexico: ISRM, 59–68.
27. Rusydy, I., Al-Huda, N., Jamaluddin, K., Sundary, D., Nugraha, G. S. (2017). Analisis Kestabilan Lereng Batu Di Jalan Raya Lhoknga Km 17, 8 Kabupaten Aceh Besar. *RISET Geologi dan Pertambangan, 27(2),* 145–155. DOI 10.14203/risetgeotam2017.v27.452.
28. Rusydy, I., Sugiyanto, D., Satrio, L., Zulfahriza,, Munandar, I. (2016). Geological aspect of slope failure and mitigation approach in Bireun - Takengon main road, Aceh Province, Indonesia. *Aceh International Journal of Science and Technology, 5(1),* 30–37. DOI 10.13170/aijst.5.1.3841.
29. Siddique, T., Alam, M. M., Mondal, M. E., Vishal, V. (2015). Slope mass rating and kinematic analysis of slopes along the national highway-58 near Jonk, Rishikesh, India. *Journal of Rock Mechanics and Geotechnical Engineering, 7(5),* 600–606. DOI 10.1016/j.jrmge.2015.06.007.
30. Sieh, K., Natawidjaja, D. (2000). Neotectonics of the Sumatran fault, Indonesia. *Journal of Geophysical Research: Solid Earth, 105(B12),* 28295–28326. DOI 10.1029/2000JB900120.
31. Singh, B., Goel, R. K. (1999). *Rock Mass Classification (A Practical Approach in Civil Engineering),* 1st edition. Oxford: Elsevler.
32. Vollmer, F. W. (1995). C program for automatic contouring of spherical orientation data using a modified Kamb method. *Computers & Geosciences, 21(1),* 31–49. DOI 10.1016/0098-3004(94)00058-3.
33. Vollmer, F. W. (2017). Orient: Spherical projection and orientation data analysis software. Retrieved March 26, 2017. Available at http://www.frederickvollmer.com/orient/.
34. Wyllie, D. C., Mah, C. W. (2004). *Rock Slope Engineering (Civil and Mining),* 4th edition. London and New York: Spon Press.